Mater. Res. Soc. Symp. Proc. Vol. 1258 © 2010 Materials Research Society 1258-P02-05

Influence of silicon doping on the SA-MOVPE of InAs nanowires

Kamil Sladek [1], Andreas Penz [1], Karl Weis [1], Stephan Wirths [1], Christian Volk [1], Shima Alagha [1], Masashi Akabori [2,1], Steffi Lenk [1], Martina Luysberg [3], Hans Lueth [1], Hilde Hardtdegen [1], Thomas Schaepers [1], and Detlev Gruetzmacher [1]

[1] Institute of Bio- and Nanosystems (IBN-1), Forschungszentrum Juelich, Juelich, Germany.

[2] Japan Advanced Institute of Science and Technology (JAIST), Center for Nano Materials and Technology (CNMT), Nomi, Japan.

[3] Institute of Solid State Physics (IFF), Forschungszentrum Juelich, Juelich, Germany.

ABSTRACT

The influence of Si-doping on the growth and material characteristics of InAs nanowires deposited by metal-organic vapor phase epitaxy (MOVPE) was investigated. It was observed that above a certain partial pressure ratio, doping has an influence on the morphology. The nanowires exhibit better uniformity but lower height vs. diameter aspect ratio as the supply of the dopant increases. It was consistantly found that the specific conductance of the nanowires also increases. Moreover the electrical measurements showed a transition from semiconducting to metallic behavior in the case of highly doped nanowires.

INTRODUCTION

InAs nanowires are attractive for the realization of high-speed and low-power electronic devices due to the material‘s very high room temperature mobility [1,2]. Moreover if their lengths as well as their aspect ratios are sufficient, and if they are truly one-dimensional, they also can be applied for multi-gated nanodevices [3,4]. The wires are expected to be conductive even without doping, since the Fermi level is pinned at the surface and an electron accumulation layer should form. Nevertheless the InAs nanowires are not as conductive as they were predicted to be [5]. Reports on stacking faults [9,10] and possible material contamination due to their fabrication process may be the reason. Several methods of nanowire fabrication are established today. Two of the most common approaches are the catalyst assisted growth method [1,2,6-8] on the one hand and selective area growth mainly carried out by metalorganic vapor phase epitaxy (SA-MOVPE) on the other hand [9-11]. The latter approach, used in this contribution, implies higher material quality since no extrinsic impurities are inducible by metallic catalysts and less intrinsic impurities due to the higher and more suitable growth temperatures compared to catalyst assisted growth. Furthermore, since the position of each nanowire can be predefined, it provides control over the distribution and spacial density of the grown structures which also influences the growth behavior in selective area growth [12].

The aim of improving the conductivity of InAs nanowires leads to the question if doping can be applied without disturbing their growth and how it can affect their electronic characteristics. In this paper we therefore investigated the influence of doping on nanowire morphology and on nanowire conductivity.

EXPERIMENTAL DETAILS

Growth was carried out on GaAs (111)B substrates in a low-pressure MOVPE system with N_2 as the carrier gas to transport trimethylindium (TMIn) and arsine (AsH_3) into the reactor at a working pressure of 20 mbar and a total gas flow rate of 3100 sccm. The precursor partial pressures were kept constant at 0.118 and 12.9 Pa, respectively, resulting in a V/III ratio of 110. The substrates were covered by a 30 nm thin structured SiO_2 layer. The mask structure consisted of hole arrays with an about 50 nm hole diameter and 500 nm pitch which was defined by electron beam lithography using positive resists and dry etching. Directly before growth, the samples were cleaned by H_2SO_4 and rinsed in de-ionized water. Further growth details can be found in [13]. Disilane (Si_2H_6) was used for silicon doping during growth. To quantify the supply of doping species more easily a doping factor was defined, consisting of the partial pressure ratio of dopant vs. group III precursor. A ratio $p(Si_2H_6)/p(TMIn) = 7.5*10^{-5}$ was therefore set as the factor 1 and was successively varied from 0 to 500. The morphology of the grown wires was characterized by scanning electron microscopy (SEM) using a statistical evaluation of several nanowires per sample and the structure by transmission electron microscopy (TEM). For electrical characterization the nanowires were transferred onto a target which consisted of an n^+-doped silicon substrate, serving as a back-gate with a 100 nm thick dielectric layer on top (SiO_2 or Si_3N_4). Non-annealed source and drain contacts (Ti/Au) were then defined by electron beam lithography, thermal evaporation and lift-off. Four-terminal measurement setups as illustrated in figure 1 were favored in order to be able to determine the nanowire resistance independent of the contact resistance. In this setup the nanowire resistance between contacts 2 and 3 can be calculated from the fraction of measured voltage and injected current through contacts 1 and 4. The contact resistance can be estimated together with another measurement where current is injected through contacts 2 and 3. Room temperature measurements were performed using a DC probe station. For low temperature measurements down to 4 K a He-4 flow cryostat was employed.

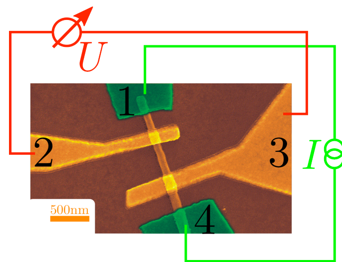

Figure 1. Colored scanning electron micrograph showing a nanowire, contacted by a four-terminal setup. The current is induced by contacts 1 and 4 while voltage is measured by contacts 2 and 3.

DISCUSSION

At first the influence of doping on nanowire morphology was investigated. The influence is shown in figure 2. As the doping factor increases the diameter of the nanowires also increases. Typically the nanowires exhibited lengths of several micrometers and diameters in the range between 70 nm and 120 nm, dependent on the doping factor. The quantitative dependence of height vs. diameter aspect ratio on doping factor is presented in figure 3. Obviously doping

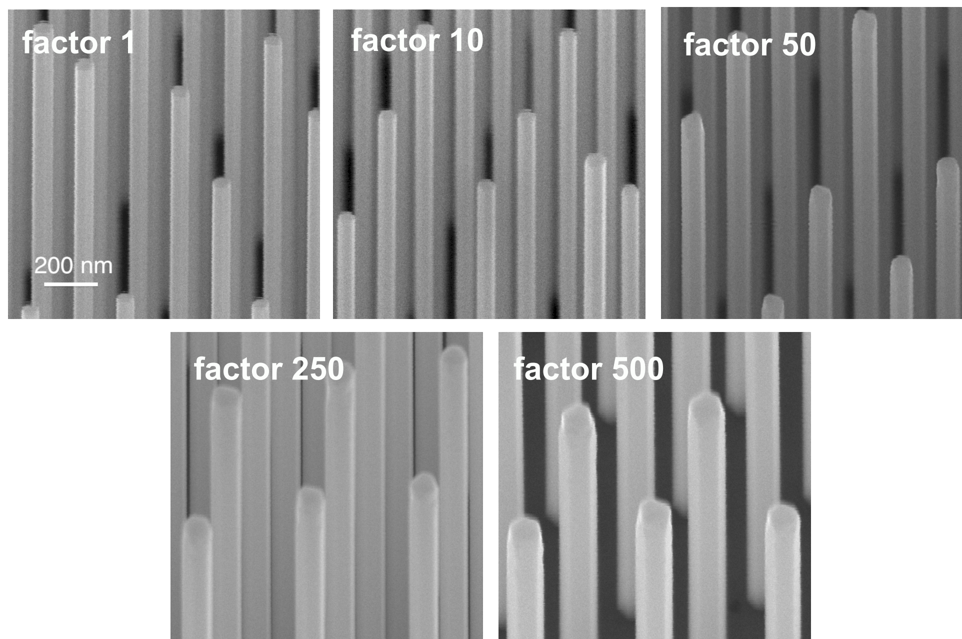

Figure 2. SEM images of InAs nanowires with different doping factors taken at the same magnification. The diameter increases visibly with the doping factor.

seems to affect the growth rates on different facet types resulting in increased radial growth and decreased axial growth. Taking into account that disilane is known to stick well on both facet types, a decrease of diffusion thus a higher incorporation probability of group III material along the (110) type side facets could be a reason for the change of growth rates. The average aspect ratio decreases nonlinearly with increasing doping factors. At the same time the standard deviation of aspect ratio also decreases as indicated by the error bars. Apparently higher doping levels lead to more homogeneous nanowire growth. As can be seen in the inset of figure 3, the more homogeneous aspect ratio is mainly due to the more homogeneous nanowire height as the doping increases. The uniformity of the nanowire diameter stays basically constant.

After morphological analysis the atomic structure was investigated. Figure 4 shows TEM images of a nanowire with the doping factor 500. Several changes in shading perpendicular to

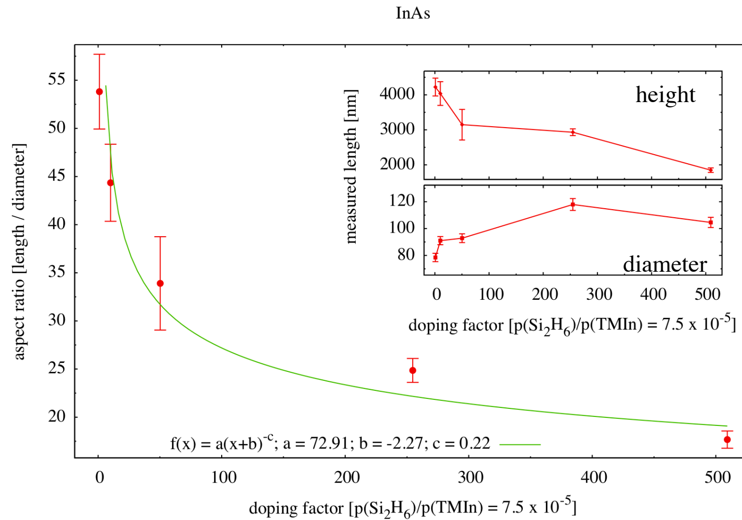

Figure 3. Averaged aspect ratio over several nanowires plotted against doping factor. Vertical bars represent standard deviations of the averaged values. A fitting curve is plotted with the corresponding function and fit parameters denoted below. The inset shows averaged heights and lengths vs. doping factor separately.

the growth direction can be observed in the left image. In the magnified area, segments of different stacking order could be observed and are highlighted in the right image. A change in the stacking order sequence corresponds to a change in the crystal structure from hexagonally to cubically close packed and vice versa. The structural changes are expected to have an influence on the electrical characteristics of the wires since polarization effects will change the electronic band structure on the scale on which they are observed [14].

The electrical characterization of the doping series shows a clear dependence between doping factor and nanowire resistivity. The left part of figure 5 shows a statistical evaluation of nanowire resistivity based on two-terminal as well as on four-terminal measurements at room temperature. Both methods, in good agreement, show up a clear trend of lower nanowire resistance towards higher doping factors. A high deviation of resistance can be observed for undoped nanowires and was confirmed by separate measurements of two nanowire ensembles.

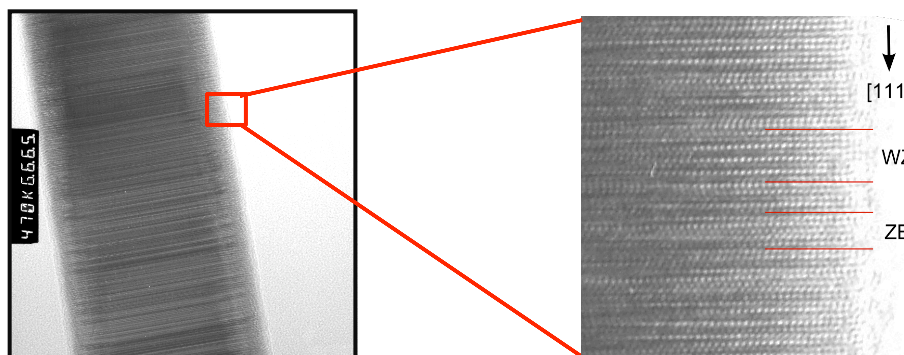

Figure 4. Transmission electron micrograph of a highly doped InAs nanowire. The magnified high-resolution area shows several stacking faults, yet the location of zincblende as well as wurtzite segments can be distinguished.

Regarding temperature dependent measurements a behavior of a degenerate semiconductor is expected especially for the thinnest InAs nanowires due to the increased surface to volume ratio and so the increased impact of surface carrier accumulation. However, nanowires with low doping factors showed semiconducting behavior in means of increased resistance at lower temperatures. Nevertheless, a decrease of the resistance with decreasing temperature could be confirmed at least for highly doped nanowires. Moreover a variation of gate voltage at different temperatures showed a transition between both regimes, as can be seen in the right part of figure 5 for a nanowire with the highest doping concentration. Starting at zero gate voltage the measurements show that the current increases with decreasing temperature due to increased carrier mobility, as expected for degenerate semiconductors. This type of behavior is decreasingly pronounced towards negative gate voltages and vanishes at a gate voltage of about -20 V. From there on towards more negative gate voltages we could observe increasingly pronounced semiconducting behavior. Assuming that the high doping concentration results in a degenerate electron gas, the transition at more negative gate voltages can be explained qualitatively by a depletion of the surface electron gas and an increased carrier depletion in the nanowire core towards a non-degenerate electron gas. In this regime the increase of the conductivity can be attributed to thermally excited carriers.

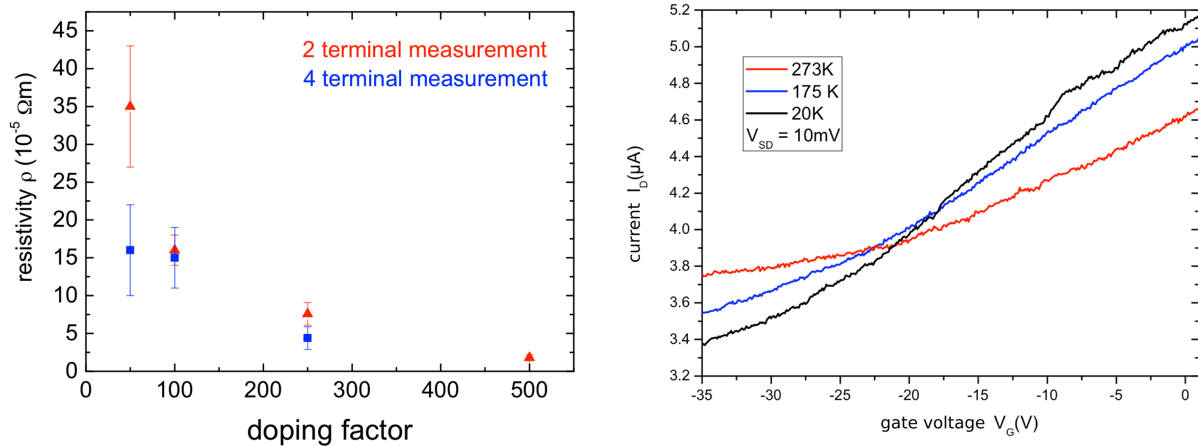

Figure 5. Left: nanowire resistivity plotted as a function of doping factor. Two-terminal and four-terminal measurements are distinguished as triangles and squares respectively. Right: current as a function of gate voltage for different temperatures. Converse temperature dependence is observed for gate voltages above and below -20 V.

CONCLUSIONS

In summary, we carried out SA-MOVPE of InAs nanowires with different doping levels on GaAs (111) B masked substrates. The influence of doping on morphology in terms of an aspect ratio decrease and a uniformity increase was shown using a statistical evaluation. Since at every doping level the wires are non-tapered and doping is applied during the entire growth time, a

homogeneous distribution of dopants inside the wire can be assumed. Further characterization needs to be done to confirm this assumption. Furthermore the general decrease of resistivity with increasing doping was confirmed by a series of two-terminal and four-terminal electrical measurements. Here, a large variation of resistance could be observed especially for undoped wires. Contrary to our expectation the relatively thin undoped nanowires showed semiconducting behavior. Possibly the internal crystallographic structure of the nanowires cause the deviation from the expected behavior. Metallic behavior was found only for the highest doped nanowires and could be influenced by applying higher gate voltages. All in all we have shown that silicon doping of InAs nanowires can be carried out in SA-MOVPE and successfully confirmed the influence of doping on nanowire conductivity in terms of increased carrier concentration.

ACKNOWLEDGMENTS

The authors thank Mr. K. Wirtz for his support in MOVPE and Dr. S. Trellenkamp for his support in electron-beam lithography. One of the authors (M. A.) was financially supported by JSPS Postdoctoral Fellowships for Research Abroad.

REFERENCES

[1] T. Bryllert, L.-E. Wernersson, L. E. Fröberg, L. Samuelson, IEEE Elec. Dev. Lett. 27, 323 (2006).
[2] S. A. Dayeh, D. P. R. Aplin, X. Zhou, P. K. L. Yu, E. T. Yu, D. Wang, Small 3, 326 (2007).
[3] C. Fasth, A. Fuhrer, M. T. Bjork, L. Samuelson, Nanoletters 5, 1487-1490 (2005).
[4] A. Pfund, I. Shorubalko, R. Leturcq, K. Ensslin, Appl. Phys. Lett., AIP, 89, 252106 (2006).
[5] A. C. Ford, J. C. Ho, Y.-L. Chueh, Y.-C. Tseng, Z. Fan, J. Guo, J. Bokor and A. Javey, Nano Letters, 9, 360-365 (2009)
[6] A. E. Hansen, M. T. Björk, C. Fasth, C. Thelander, L. Samuelson, Phys. Rev. B71, 205328 (2005) 205328.
[7] K. Hiruma, M. Yazawa, T. Katsuyama, K. Ogawa, K. Haraguchi, M. Koguchi, H. Kakibayashi, J. Appl. Phys. 77, 447 (1995).
[8] K. A. Dick, K. Deppert, T. Mårtensson, B. Mandl, L. Samuelson, W. Seifert, Nano Lett. 5, 761 (2005).
[9] K. Tomioka, J. Motohisa, S. Hara, T. Fukui, Jpn. J. Appl. Phys. 46, L1102 (2007).
[10] H. Paetzelt, V. Gottschalch, J. Bauer, G. Benndorf, G. Wagner, J. Cryst. Growth 310, 5093 (2008).
[11] K. Tomioka, P. Mohan, J. Noborisaka, S. Hara, J. Motohisa, T. Fukui, J. Cryst. Growth 298, 644 (2007).
[12] K. Sladek, V. Klinger, J. Wensorra, M. Akabori, H. Hardtdegen and D. Grützmacher, J. Cryst. Growth 312, 635 (2010).
[13] M. Akabori, K. Sladek, H. Hardtdegen, T. Schäpers and D. Grützmacher, J. Cryst. Growth, 311, 3813 (2009).
[14] S. A. Dayeh, Semiconductor Science and Technology 25, 024004 (2010).